The Astronomical Journal, 130:1635–1639, 2005 October


# A $^{12}$CO $J = 4 \rightarrow 3$ HIGH-VELOCITY CLOUD IN THE LARGE MAGELLANIC CLOUD

Sungeun Kim,[1] Wilfred Walsh,[2] Kecheng Xiao,[2] and Adair P. Lane[2]

*Received 2005 April 13; accepted 2005 June 17*

## ABSTRACT

We present Antarctic Submillimeter Telescope and Remote Observatory observations of $^{12}$CO $J = 4 \rightarrow 3$ and $^{12}$[C I] emission in the 30 Doradus complex in the Large Magellanic Cloud. We detected strong $^{12}$CO $J = 4 \rightarrow 3$ emission toward R140, a multiple system of Wolf-Rayet stars located on the rim of the expanding H II shell surrounding the R136 cluster. We also detected a high-velocity gas component as a separate feature in the $^{12}$CO $J = 4 \rightarrow 3$ spectrum. This component probably originates from molecular material accelerated as a result of the combined motion induced by the stellar winds and explosions of supernovae, including several fast-expanding H II shells in the complex. The lower limit on the total kinetic energy of the atomic and molecular gas component is $\sim 2 \times 10^{51}$ ergs, suggesting that this comprises only 20% of the total kinetic energy contained in the H II complex structure.

*Key words:* ISM: atoms — ISM: general — ISM: molecules — Magellanic Clouds

## 1. INTRODUCTION

The most luminous example of a starburst region in the Local Group is 30 Doradus in the Large Magellanic Cloud (LMC); its core R136 is one of the "super star clusters" (SSCs). The giant H II region complex extends for more than 100 pc (Chu & Kennicutt 1994). The massive stars in the core of R136 were formed about 1–2 Myr ago (Massey & Hunter 1998). This starburst region has multiple stellar generations (Rubio et al. 1998; Walborn et al. 2002), and *Hubble Space Telescope* (*HST*) NICMOS observations have identified at least 20 pre-main-sequence stars embedded in the nebular filaments (Brandner et al. 2001). The interaction of massive stars and their interstellar environment in this region has been perfectly illustrated by the *Spitzer Space Telescope* early release observations of 30 Doradus in the LMC.[3] This complex has received a great deal of attention and has been investigated at various wavelengths. For instance, X-ray emission was mapped by Wang & Helfand (1991) and Wang (1999), molecular emission was observed by Johansson et al. (1998), and infrared embedded sources were studied as an example of a current star formation episode by Rubio et al. (1998). Lazendic et al. (2003) identified supernovae candidates in the 30 Doradus complex.

At a distance of 55 kpc (Feast 1991), the LMC can be mapped with a high spatial resolution in mid-$J$ excitation of $^{12}$CO lines even by a small telescope. Recent [C I] and $^{12}$CO $J = 4 \rightarrow 3$ studies of the N159 and N160 complexes in the LMC by Bolatto et al. (1999, 2000) have elucidated the condition of the atomic and molecular medium in the early stages of star formation. In this paper, we report the detection of high-velocity $^{12}$CO $J = 4 \rightarrow 3$ emission toward the 30 Doradus complex in the LMC. Observations of such a mid-$J$ excitation of $^{12}$CO lines in the 30 Doradus region provide a better understanding of the relative distribution of molecular, atomic, and ionized gas in metal-poor galaxies.

## 2. OBSERVATIONS

The observations were carried out during the austral winter season of 2002 at the Antarctic Submillimeter Telescope and Remote Observatory (AST/RO), located at 2847 m altitude at the Amundsen-Scott South Pole Station. AST/RO is a 1.7 m diameter, offset Gregorian telescope that is capable of observing at wavelengths between 200 $\mu$m and 1.3 mm (Stark et al. 2001). This site is very dry and is therefore well suited for submillimeter observations (Chamberlin et al. 1997). We used a dual-channel superconductor-insulator-superconductor (SIS) waveguide receiver (Walker et al. 1992; Honingh et al. 1997) for simultaneous observations at 461–492 and 807 GHz. Two acousto-optical spectrometers (AOSs; Schieder et al. 1989) were used as back ends. The AOSs had a 1.07 MHz resolution and a 0.75 GHz effective bandwidth, resulting in velocity resolutions of 0.65 km s$^{-1}$ at 461 GHz and 0.37 km s$^{-1}$ at 807 GHz. The data were smoothed to a uniform velocity resolution of 1 km s$^{-1}$. The high-frequency observations were made with the $^{12}$CO $J = 7 \rightarrow 6$ line in the lower sideband (LSB). Since the intermediate frequency of the AST/RO system is 1.5 GHz, the $^3P_2 \rightarrow {}^3P_1$ line of [C I] line appears in the upper sideband (USB) and is superposed on the observed LSB spectrum. The local oscillator frequency was chosen so that the nominal line centers appear separated by 100 km s$^{-1}$ in the double-sideband spectra. A third AOS, used for only a few spectra, had a 0.031 MHz resolution and a 0.25 GHz bandwidth. Atmosphere-corrected system temperatures ranged from 320 to 390 K at 461–492 GHz and 1050 to 1190 K at 807 GHz.

Emission from the $^{12}$CO $J = 7 \rightarrow 6$ lines at 806.6517 GHz was mapped over a $7' \times 11'$ region centered on R.A. $= 5^{\rm h}38^{\rm m}45^{\rm s}$, decl. $= -69^\circ 04' 45''$ (J2000.0) with $1'$ spacing and a beam size of $58''$. Observation time at each position was typically 13 minutes. Either the [C I] line at 492.262 GHz or the $^{12}$CO $J = 4 \rightarrow 3$ line at 461.041 GHz was observed simultaneously with beam sizes of $103''$–$109''$. We used the standard chopper wheel calibration technique, implemented at AST/RO by way of regular observations (every few minutes) of the sky and two blackbody loads of known temperature (Stark et al. 2001). Atmospheric transmission was monitored by regular sky dips, and known, bright sources were observed every few hours. The intensity calibration errors were estimated to be $\pm 40\%$.

## 3. RESULTS

Figure 1 presents the $^{12}$CO $J = 4 \rightarrow 3$ line emission taken with the AST/RO with the spatial coverage of the individual pointings. We detected strong $^{12}$CO $J = 4 \rightarrow 3$ emission at R.A. $= 5^{\rm h}38^{\rm m}49\overset{\rm s}{.}7$, decl. $= -69^\circ 04' 4\overset{''}{.}7$ (J2000.0) and to the north of the R136 cluster in the 30 Doradus region. From the comparisons

[1] Department of Astronomy and Space Science, Sejong University, KwangJin-gu, KunJa-dong 98, Seoul 143-747, South Korea; skim@arcsec.sejong.ac.kr.

[2] Harvard-Smithsonian Center for Astrophysics, 60 Garden Street, MS-12, Cambridge, MA 02138; wwalsh@cfa.harvard.edu, kxiao@cfa.harvard.edu, adair@cfa.harvard.edu.

[3] See http://www.spitzer.caltech.edu/media/releases/ssc2004-01/index.shtml.

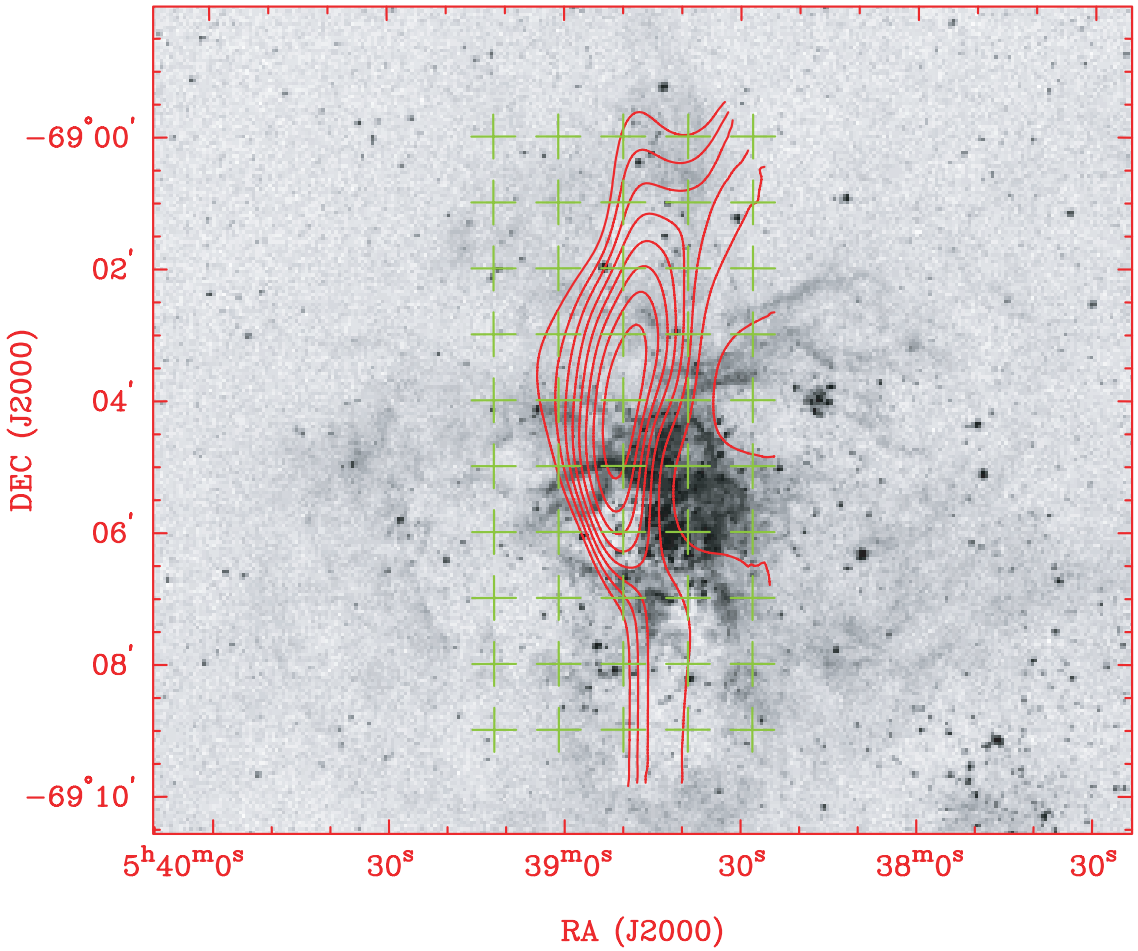


FIG. 1.—Integrated intensity contour map of $^{12}$CO $J = 4 \rightarrow 3$ emission observed with the AST/RO telescope. The coverage is plotted for the individual pointings. The gray scale is the Digitized Sky Survey image of the 30 Doradus complex. The range of velocity integration covers the velocity range of $V_{LSR} = 240$–$260$ km s$^{-1}$. The lowest contour is 0.8 K km s$^{-1}$, and the contours increase by 0.4 K km s$^{-1}$.

of $^{12}$CO $J = 1 \rightarrow 0$ (Johansson et al. 1998; Fukui et al. 1999) and $^{12}$CO $J = 4 \rightarrow 3$ maps, we have found that the peak of $^{12}$CO $J = 4 \rightarrow 3$ emission is located at 2′ northwest of the peak of $^{12}$CO $J = 1 \rightarrow 0$ emission.

The spectrum of the peak $^{12}$CO $J = 4 \rightarrow 3$ emission is displayed in Figure 2. The $^{12}$CO $J = 4 \rightarrow 3$ emission lines appear at $V_{LSR} = 249.6 \pm 0.3$ km s$^{-1}$ and $V_{LSR} = 302.0 \pm 0.2$ km s$^{-1}$. Fitting a Gaussian curve to the main velocity component of $^{12}$CO $J = 4 \rightarrow 3$ emission gives a velocity of $V_{LSR} = 249.6$ km s$^{-1}$. This systemic velocity is similar to that of $^{12}$CO $J = 1 \rightarrow 0$ emission, $V_{LSR} = 249.5$ km s$^{-1}$ (Mizuno et al. 2001) and $V_{LSR} = 249.7$ km s$^{-1}$ (Johansson et al. 1998). However, both observations of $^{12}$CO $J = 1 \rightarrow 0$ emission by Johansson et al. (1998) and Mizuno et al. (2001) show only a single component of the emission at $V_{LSR} \sim 250$ km s$^{-1}$. The peak brightness temperature of the $^{12}$CO $J = 4 \rightarrow 3$ main-beam emission is $T_{MB} = 0.542 \pm 0.1$ K. The integrated intensity of the emission is $3.5 \pm 0.2$ K km s$^{-1}$. Since the forward efficiency for AST/RO is ~0.97–1.0 (Stark et al. 2001), we assume this to be identical to the main-beam efficiency. These parameters are summarized in Table 1. The luminosity $L_{CO}$ of $^{12}$CO $J = 4 \rightarrow 3$ emission is about $3.82 \times 10^3$ $L_\odot$ by adopting the size of 75 pc × 135 pc and is similar to that of the Sgr A complex in the Galactic center (Kim et al. 2002).

No $^{12}$CO $J = 7 \rightarrow 6$ emission line was detected in the position of the peak $^{12}$CO $J = 4 \rightarrow 3$ emission as seen in Figure 2. [C I] 492 GHz emission and [C I] 809 GHz emission lines were also not detected. We derived the upper limit for the [C I] 492 GHz emission integrated intensity as $\sim 0.5 \pm 0.1$ K km s$^{-1}$ within this region where the $^{12}$CO $J = 4 \rightarrow 3$ emission was detected. Here the upper limit was defined by 3 $\sigma$ rms noise, and the rms noise in the integrated intensity of a nondetected region was calculated by $(n_{chan})^{1/2} \Delta v_{chan} T_{rms}$, where $n_{chan}$ is twice the full width at half-maximum (FWHM) of the line in numbers of channels, and $\Delta v$ is the channel separation in km s$^{-1}$. The uncertainty in this upper limit may be increased by noise fluctuation.

The integrated H I map of the 30 Doradus complex shows a clear depression that corresponds to the $^{12}$CO $J = 4 \rightarrow 3$ emitting gas. Interestingly, as shown in Figures 3 and 4, the H I shell encompasses the $^{12}$CO $J = 4 \rightarrow 3$ emitting gas as well as the whole giant H II complex. The expansion of this H I shell is uniform and visualized in the position-velocity plot in Figure 5. Its systemic velocity, determined from the H I velocities at the rim of the shell, is $V_{LSR} = 254$–$264$ km s$^{-1}$. Referenced to this systemic velocity, the expanding hemisphere of the neutral gas shell has an expansion velocity of $18 \pm 2.0$ km s$^{-1}$. The H I emission cube for the 30 Doradus complex has been extracted from the LMC H I combined Australia Telescope Compact Array (ATCA; Kim et al. 1998) and Parkes surveys (Kim et al. 2003).

It is not yet possible to determine the $^{12}$CO $J = 4 \rightarrow 3$ emission concentrations within the entire 30 Doradus complex in

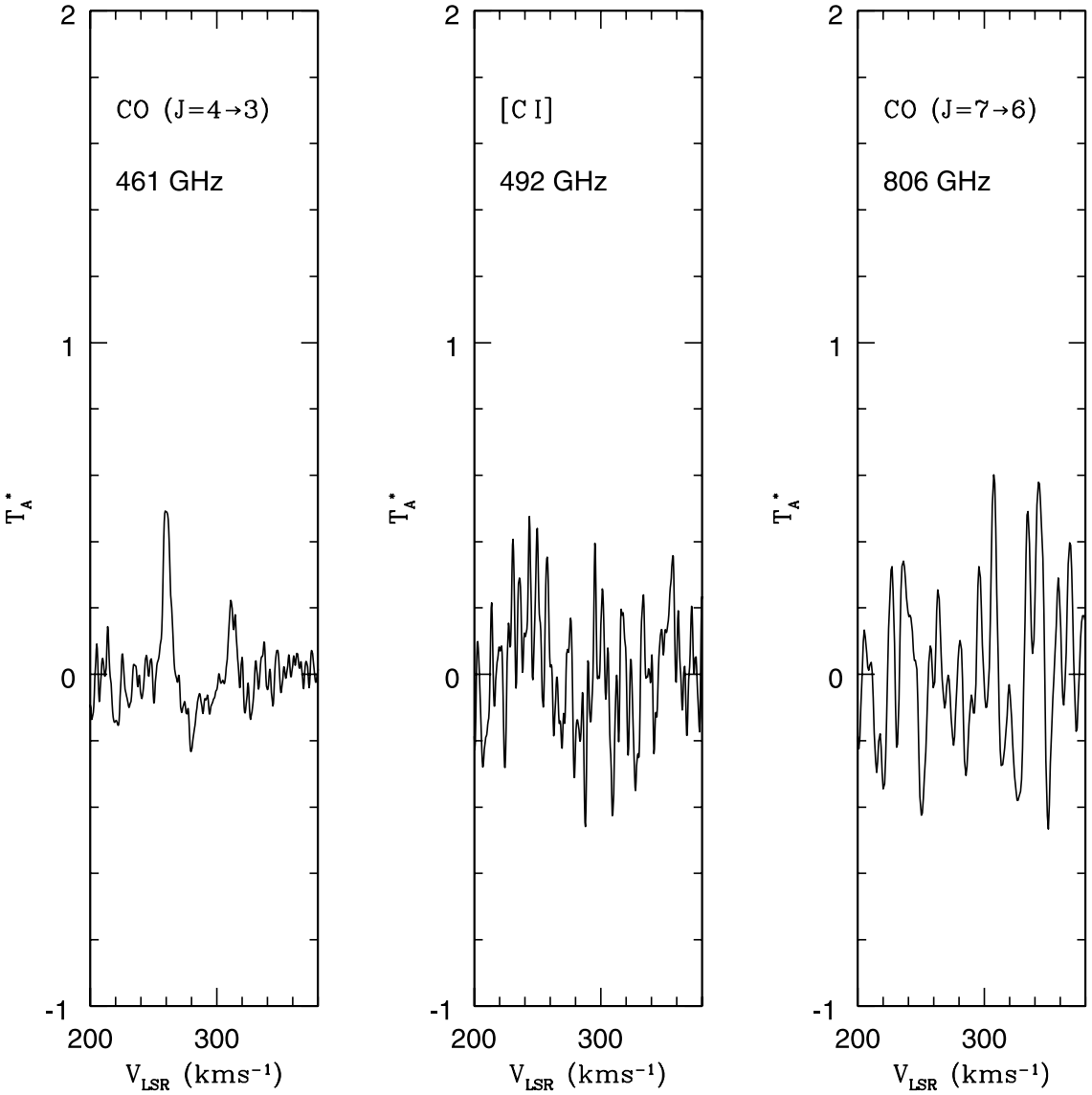


FIG. 2.—The $^{12}$CO $J = 4 \rightarrow 3$, $^{12}$[C I] 492 GHz, and $^{12}$CO $J = 7 \rightarrow 6$ spectra observed toward the peak of the $^{12}$CO $J = 4 \rightarrow 3$ emission in the 30 Doradus complex. Note the second, high-velocity peak at 302 km s$^{-1}$ in the $^{12}$CO $J = 4 \rightarrow 3$ spectrum. The present spectra were Hanning-smoothed.

the LMC with our limited spatial coverage. However, our results show that a dense and warm molecular cloud in fact resides inside the H I shell, not on the H I shell itself. This picture is substantially different from that seen in the N44 complex of the LMC (Kim et al. 2004), where the warm and dense molecular cloud is located on the rim of the H I shell. The observed $^{12}$CO $J = 4 \rightarrow 3$ emission indicates that the neutral interstellar medium toward the rim of the giant H II shell surrounding LH47 in the N44 complex is very dense and warm, since the $^{12}$CO $J = 4 \rightarrow 3$ transition requires $T > 50$ K and $n \sim 10^5$ cm$^{-3}$ (Bolatto et al. 2000; Cecchi-Pestellini et al. 2001; Zhang et al. 2001; Kim et al. 2002). However, the mid-$J$ excitation $^{12}$CO lines can also be an indicator of temperature rather than of the total amount of molecular gas (Willacy et al. 2002).

It is found that the $^{12}$CO $J = 4 \rightarrow 3$ emitting cloud is located on the northern H II filaments surrounding the R136 cluster. Previous studies by Rubio et al. (1998) and Johansson et al. (1998) indicated that the massive molecular clouds are present to the north of R136 cluster. This region is evidently forming stars triggered by the energetic stellar winds from the R136 cluster (Walborn et al. 2002). Notably, the peak of $^{12}$CO $J = 4 \rightarrow 3$ emission corresponds to the R140 multiple system in the 30

TABLE 1
OBSERVED LINE PARAMETERS

| Line | $T_{MB}$ (K) | $V_{LSR}$ (km s$^{-1}$) | $\Delta V$ (km s$^{-1}$) | $\int T_{MB}\, dV$ (K km s$^{-1}$) |
|---|---|---|---|---|
| 461 GHz $^{12}$CO $J = 4 \rightarrow 3$ ..... | 0.542 ± 0.1 | 249.61 ± 0.1 | 6.195 ± 1.3 | 3.57 ± 0.2 |
| 461 GHz $^{12}$CO $J = 4 \rightarrow 3$[a] ..... | 0.16 | 302.0 | 5.1 | 1.6 |
| 115 GHz $^{12}$CO $J = 1 \rightarrow 0$..... | 1.5 | 249.7 | 8.3 | 13 |

[a] High-velocity component.

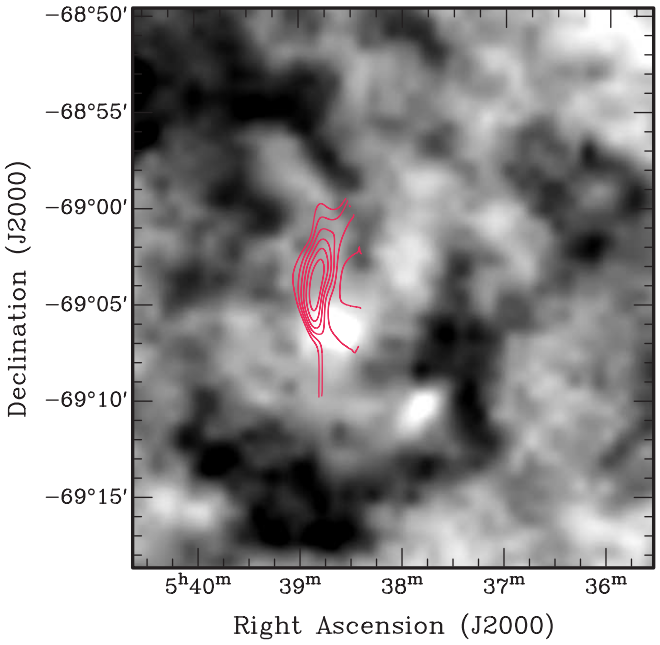


FIG. 3.—ATCA+Parkes H I image of the 30 Doradus complex in the LMC from Kim et al. (2003). It is clearly seen that the $^{12}$CO $J = 4 \rightarrow 3$ emitting cloud is located in the shell.

Doradus nebula. The R140 multiple system in the nebula has been reported to have at least three Wolf-Rayet stars by Moffat et al. (1987). A high-velocity $^{12}$CO $J = 4 \rightarrow 3$ gas ($V_{\rm LSR} \approx$ 302 km s$^{-1}$) is clearly visible in the region where the peak of $^{12}$CO $J = 4 \rightarrow 3$ emission is detected. The brightness temperature of this high-velocity $^{12}$CO $J = 4 \rightarrow 3$ gas, $T_{\rm MB} \approx 0.21 \pm 0.09$ K, is fainter than that of the systemic one. The FWHM of this fainter $^{12}$CO $J = 4 \rightarrow 3$ emission is approximately 7 km s$^{-1}$ and similar to that of the systemic component, $6.1 \pm 1.0$ km s$^{-1}$. Note that a mosaic of H$\alpha$ echellogram observations taken by

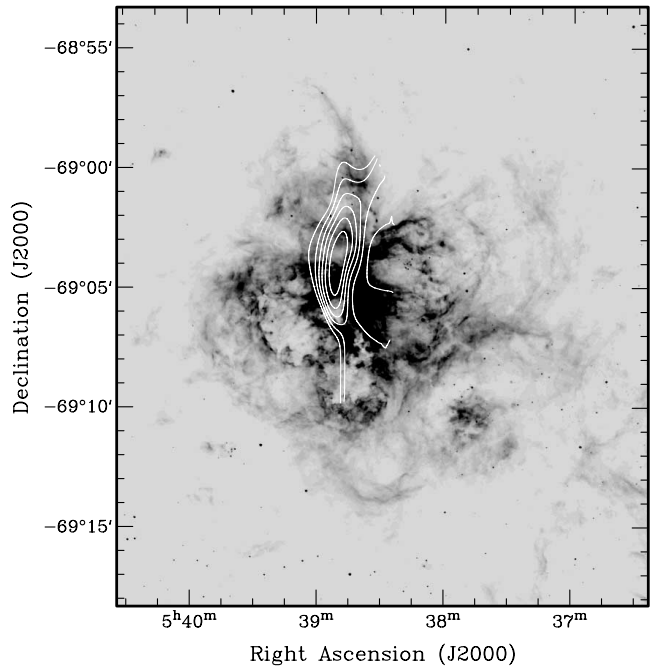


FIG. 4.—The $^{12}$CO $J = 4 \rightarrow 3$ emission overlaid on the H$\alpha$ image (reprinted with permission from C. Smith) of the 30 Doradus complex in the LMC. The whole complex is encompassed by the H I shell seen in Fig. 3.

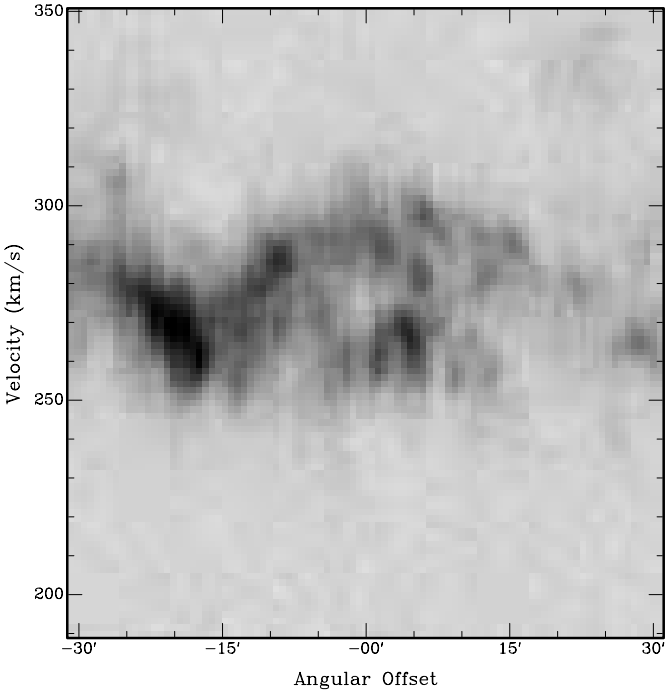


FIG. 5.—Position-velocity diagram of the H I shell (Kim et al. 2003) along strips crossing the peak $^{12}$CO $J = 4 \rightarrow 3$ emission. The unit of the H I velocity is in heliocentric velocity, $V_{\rm Hel} = V_{\rm LSR} + 16$ km s$^{-1}$.

Chu & Kennicutt (1994) shows several discrete high-velocity features in which the high-velocity component of $^{12}$CO $J = 4 \rightarrow 3$ emission is detected.

## 4. DISCUSSION

The mass of the $^{12}$CO $J = 4 \rightarrow 3$ emitting cloud can be derived using the equation $M_{\rm cloud} = \mu m({\rm H_2}) \Sigma D^2 \Omega N({\rm H_2})$ and assuming the LTE. $D$ is the distance of the LMC, $\Omega$ is the solid angle subtended, $m({\rm H_2})$ is the $H_2$ molecular mass, and $\mu$ is the mean molecular weight assumed to be 1.36 by taking into account the relative helium abundance in mass. The $H_2$ column density, $N({\rm H_2})$, can be derived from the integrated $^{12}$CO $J = 1 \rightarrow 0$ intensity $\sim$5.1 (in K km s$^{-1}$ ) and the CO-$H_2$ conversion factor $X = [N({\rm H_2})/I_{\rm CO}] \sim (9 \pm 4) \times 10^{20}$ cm$^{-2}$ (K km s$^{-1}$)$^{-1}$ (Mizuno et al. 2001). Then, the mass of molecular gas traced in the $^{12}$CO $J = 4 \rightarrow 3$ emission is about $(6.6 \pm 2.9) \times 10^4\ M_\odot$. We estimate the mass of the high-velocity molecular cloud to be $(2.6 \pm 1.6) \times 10^4\ M_\odot$ by using the $T_{\rm MB}$ line ratio of the $^{12}$CO $J = 4 \rightarrow 3$ emission at $V_{\rm LSR} \sim 249.6$ km s$^{-1}$ and $V_{\rm LSR} \sim 302$ km s$^{-1}$. The mass fraction of this high-velocity gas in the parent giant molecular cloud is about 30%. Thus, the kinetic energy of the high-velocity molecular cloud is approximately $(7.5 \pm 0.6) \times 10^{50}$ ergs. This indicates a lower limit on the kinetic energy due to the solid angle subtended by $^{12}$CO $J = 4 \rightarrow 3$ emission.

The expanding H I shell encompassing the giant H II regions and shells extends 20′ on the sky, which is about 300 pc across at the distance of the LMC. H I material associated with the shell shows a typical expansion structure in the position-velocity diagram (Fig. 5) along strips crossing the peak $^{12}$CO $J = 4 \rightarrow 3$ emission. The H I mass associated with accelerated gas from the shell can be derived using the average column density of the inner sphere of the H I shell, to be $4 \times 10^5\ M_\odot$. The kinetic energy of the H I shell is therefore about $1.3 \times 10^{51}$ ergs. Compared to the total kinetic energy of $\sim 1 \times 10^{52}$ ergs contained in the gas of the 30 Doradus core (Chu & Kennicutt 1994), the lower limit of

the total kinetic energy of the atomic and molecular gas component is $\sim 2 \times 10^{51}$ ergs. This amounts to 20% of the total kinetic energy produced by the stellar winds and/or supernovae explosions in the 30 Doradus complex in the LMC. The lower limit of the kinetic energy of the molecular gas component is slightly smaller than the kinetic energy of the H I shell. While more data are needed to confirm the extension of this source, this measurement suggests that the results of the study of the N44 complex in the LMC, where the lower limit of the kinetic energy of the high-velocity gas observed in the $^{12}$CO $J = 4 \rightarrow 3$ emission was at least fourfold higher than that of the H I shell (Kim et al. 2004), do not rule out alternative scenarios. To pursue this further, we need more observational data on the molecular outflow within the shell.

We thank A. A. Stark (AST/RO PI) for his support of this project and helpful discussion; C. Walker and his SORAL receiver group at the University of Arizona; J. Kooi and R. Chamberlin of Caltech, G. Wright of Antiope Associates, and K. Jacobs of U. Köln for their work on the instrumentation; and R. Schieder, J. Stutzki, and colleagues at U. Köln for their AOSs. We thank C. Smith and J. Lazendic for providing the H$\alpha$ image. We thank the anonymous referee for helpful comments. We also thank LMC HI ATCA+Parkes survey project team members. This research was in part supported by NSF grant number OPP-0126090. S. K. was supported in part by the Korea Science & Engineering Foundation (KOSEF) under a cooperative agreement with the Astrophysical Research Center of the Structure and Evolution of the Cosmos (ARCSEC).

## REFERENCES

Bolatto, A., Jackson, J. M., Israel, F. P., Zhang, X., & Kim, S. 2000, ApJ, 545, 234
Bolatto, A., Jackson, J. M., Wilson, C. D., & Zhang, X. 1999, in Proc. IAU Symp. 190, New Views of the Magellanic Clouds, ed. Y.-H. Chu et al. (San Francisco: ASP), 128
Brandner, W., Grebel, E. K., Barba, R. H., Walborn, N. R., & Moneti, A. 2001, AJ, 122, 858
Cecchi-Pestellini, C., Casu, S., & Scappini, F. 2001, MNRAS, 326, 1255
Chamberlin, R., Lane, A. P., & Stark, A. A. 1997, ApJ, 476, 428
Chu, Y.-H., & Kennicutt, R. C., Jr. 1994, ApJ, 425, 720
Feast, M. W. 1991, in Proc. IAU Symp. 148, The Magellanic Clouds, ed. R. Haynes & D. Milne (Dordrecht: Kluwer), 1
Fukui, Y., et al. 1999, PASJ, 51, 745
Honingh, C. E., Haas, S., Hottgenroth, D., Jacobs, K., & Stutzki, J. 1997, IEEE Trans. Appl. Superconductivity, 7, 2582
Johansson, L. E. B., et al. 1998, A&A, 331, 857
Kim, S., Martin, C., Stark, A. A., & Lane, A. P. 2002, ApJ, 580, 896
Kim, S., Staveley-Smith, L., Dopita, M. A., Freeman, K. C., Sault, R. J., Kesteven, M. J., & McConnell, D. 1998, ApJ, 503, 674
Kim, S., Staveley-Smith, L., Dopita, M. A., Sault, R. J., Freeman, K. C., Lee, Y., & Chu, Y.-H. 2003, ApJS, 148, 473
Kim, S., Walsh, W., & Xiao, K. 2004, ApJ, 616, 865
Lazendic, J. S., Dickel, J. R., & Jones, P. A. 2003, ApJ, 596, 287
Massey, P., & Hunter, D. A. 1998, ApJ, 493, 180
Mizuno, N., et al. 2001, PASJ, 53, 971
Moffat, A. F. J., Niemela, V. S., Philips, M. M., Chu, Y.-H., & Seggewiss, W. 1987, ApJ, 312, 612
Rubio, M., Barba, R. H., Walborn, N. R., Probst, R. G., Garcia, J., & Roth, M. R. 1998, AJ, 116, 1708
Schieder, R., Tolls, V., & Winnewisser, G. 1989, Exp. Astron., 1, 101
Stark, A. A., et al. 2001, PASP, 113, 567
Walborn, N. R., Maiz-Apellaniz, J., & Barba, R. H. 2002, AJ, 124, 1601
Walker, C. K., Kooi, J. W., Chan, M., LeDuc, H. G., Schaffer, P. L., Carlstrom, J. E., & Phillips, T. G. 1992, Int. J. Infrared Millimeter Waves, 13, 785
Wang, Q., & Helfand, D. J. 1991, ApJ, 373, 497
Wang, Q. D. 1999, ApJ, 510, L139
Willacy, K., Langer, W. D., & Allen, M. 2002, ApJ, 573, L119
Zhang, X., Lee, Y., Bolatto, A., & Stark, A. A. 2001, ApJ, 553, 274